DATA TRANSFORMATIONS FOR IMPROVED DISPLAY AND FITTING OF SINGLE-CHANNEL DWELL TIME HISTOGRAMS

F. J. SIGWORTH AND S. M. SINE
Department of Physiology, Yale University School of Medicine, New Haven, Connecticut 06510

ABSTRACT A. L. Blatz and K. L. Magleby (1986*a*. *J. Physiol. [Lond.]*. 378:141–174) have demonstrated the usefulness of plotting histograms with a logarithmic time axis to display the distributions of dwell times from recordings of single ionic channels. We derive here the probability density function (pdf) corresponding to logarithmically binned histograms. Plotted on a logarithmic time scale the pdf is a peaked function with an invariant width; this and other properties of the pdf, coupled with a variance-stabilizing (square root) transformation for the ordinate, greatly simplify the interpretation and manual fitting of distributions containing multiple exponential components. We have also examined the statistical errors in estimation, by the maximum-likelihood method, of kinetic parameters from logarithmically binned data. Using binned data greatly accelerates the fitting procedure and introduces significant errors only for bins spaced more widely than 8–16 per decade.

INTRODUCTION

The rates of known conformational transitions in proteins span many orders of magnitude, from picoseconds to hours, reflecting the fact that transition rates depend exponentially on underlying energy differences. It is therefore natural to plot relaxation data on a logarithmic time scale, as was done by Austin et al. (1975) in their study of optical absorbance changes in myoglobin over a time scale of 2 μs to 1 ks. Blatz and Magleby (1986*a*, *b*) have recently shown the utility of a similar log-log representation for dwell-time distributions from single-channel recordings where the time constants are spread over several orders of magnitude. McManus et al. (1987) have also considered the bias introduced into estimates of fitted parameters by finite sampling intervals and binning. We present here an alternative, direct display method for histograms of constant logarithmic bin width and derive the corresponding probability density function (pdf). We also present an improved procedure for maximum-likelihood estimation of kinetic parameters from binned data, and we report the results of simulations to test the performance of this procedure.

Fig. 1 *A* illustrates the limitations of the traditional linear histogram in displaying a dwell-time distribution having two exponential components. One component is well resolved on the time scale chosen for this plot; it comprises 70% of the events and has a time constant of 10 ms. The remaining 30% of the events belong to a component with a 100-ms time constant which is hardly visible on this time scale. The other parts of Fig. 1 show the same simulated data (5,120 events) and corresponding theoretical curves plotted on logarithmic time scales. Part *B* shows the representation introduced by Blatz and Magleby (1986*a*). Here the probability density, estimated by dividing the number of events in each bin by the bin width, is plotted on a log-log scale along with a log-log plot of the theoretical pdf. Parts *C* and *D* show the new representations to be considered in this paper, where the number of events in each bin (there are 10 equally spaced bins per decade) is plotted on a linear (*C*) or square-root ordinate (*D*). Superimposed on the histograms are the appropriately transformed, theoretical pdfs. Under the transformation to a logarithmic abscissa, the pdf corresponding to each exponential component of the distribution is not monotonic but has a peak at the value of the time constant. The unusual shape of the pdf can be understood from the fact that the bins at very short times are narrow and so collect few events, whereas at long times the frequency of events decreases exponentially, much more quickly than the increase in bin width. Thus a maximum is to be expected in the vicinity of the time constant of the distribution.

DISPLAY OF DISTRIBUTIONS

Linear Histograms

For comparison with the theory for the logarithmic histograms, we first review the theory of the traditional linear histogram (see for example Colquhoun and Hawkes, 1983). A set of bins is defined as having a width δt and starting values belonging to a sequence of times t_i. Entries are made in the bins according to the dwell times observed, such that the number of entries n_i in the ith bin is the number of events having durations t that satisfy

$$t_i \le t < t_i + \delta t.$$

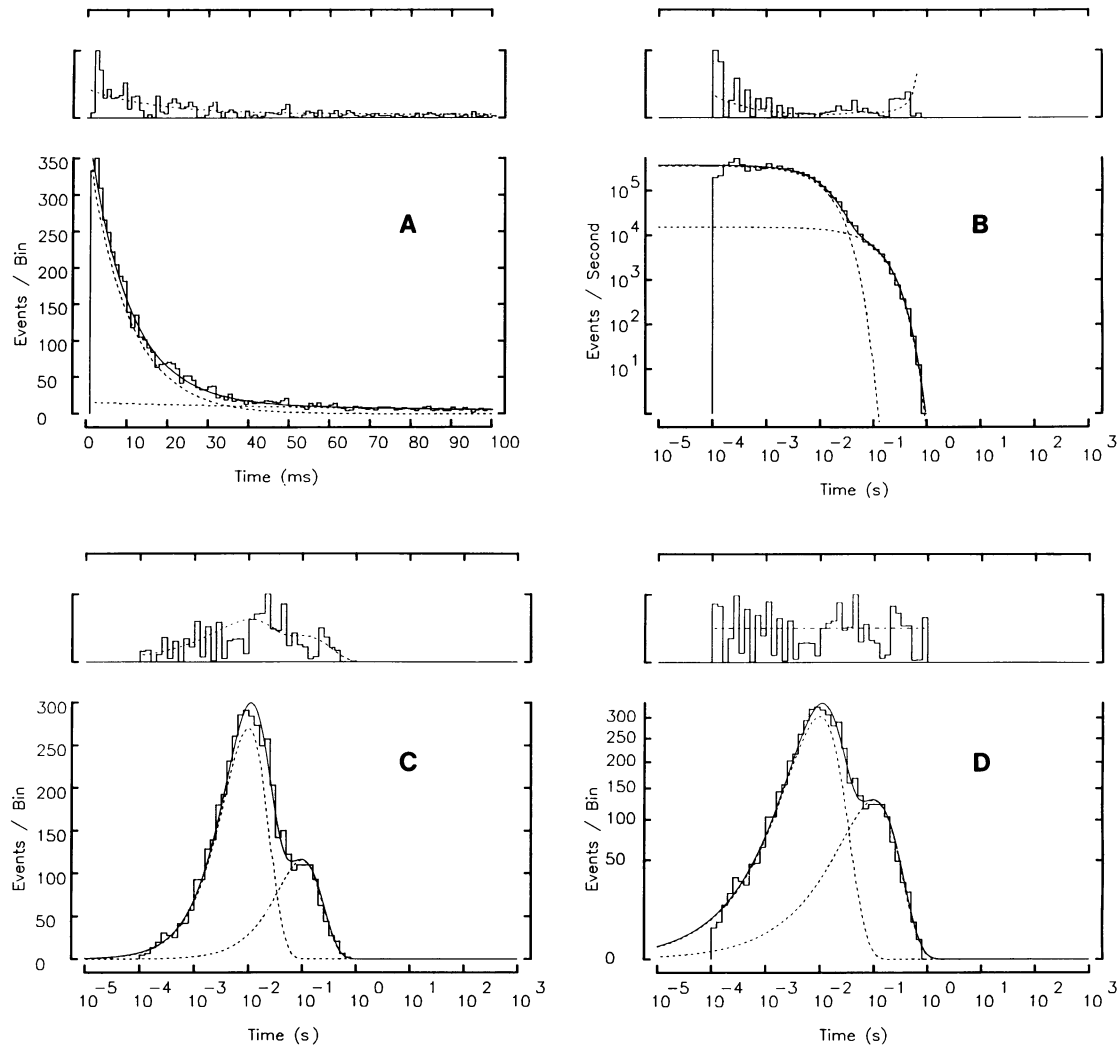

FIGURE 1 Four representations of a dwell-time distribution with two exponential components. 5,120 random numbers were generated according to a distribution with time constants of 10 ms (70% of the events) and 100 ms (30%) and binned for display as histograms in the lower panel of each part of the figure. Superimposed are the theoretical probability density functions for each component (*dashed curves*) and their sum (*continuous curve*). In each part of the figure the upper panel plots the absolute value of the deviation of the height of each bin from the theoretical curve, with dashed curves showing the expectation value of the standard deviation for each bin. The upper panels were plotted with vertical expansion factors of 2.1, 5.4, 3.1, and 4.9, respectively. (*A*) Linear histogram. Events are collected into bins of 1 ms width and plotted on a linear scale. The 100-ms component has a very small amplitude in this plot. (*B*) Log-log display with variable-width (logarithmic) binning. The number of entries in each bin is divided by the bin width to obtain a probability density in events/s which is plotted on the ordinate. (*C*) Direct display of a logarithmic histogram. Events are collected into bins of width $\delta x = 0.2$, and superimposed on the histogram is the sum of two functions as in Eq. 11. (*D*) Square-root ordinate display of a logarithmic histogram as in *C*. Note that the scatter about the theoretical curve is constant throughout the display.

In order to compare the histogram values n_i with a kinetic theory, a pdf is computed from the theory. The pdf is defined as a limit of the probability that the random open time **t** falls in a range centered on t,

$$f(t) = \lim_{h \to 0} \frac{\text{Prob}(t - h/2 < \mathbf{t} < t + h/2)}{h}.$$

Thus if the bin width δt is made sufficiently small, the expected values of n_i become proportional to the value of f at the center of the bin,

$$n_i \simeq N \delta t f(t_i + \delta t/2), \quad (1)$$

where N is the total number of events entered into the histogram.

Single Exponential Distribution. The probability distribution function is defined as the probability that a random dwell time **t** falls below a given value t,

$$F(t) = \text{Prob}\ (\mathbf{t} < t).$$

A kinetic process involving a single transition step gives rise to dwell times having an exponential distribution. The probability distribution function for such a process with a

mean dwell time τ is

$$F(t) = 1 - \exp(-t/\tau), \tag{2}$$

The probability density function (pdf) is the derivative of the distribution function,

$$f(t) = \frac{\mathrm{d}}{\mathrm{d}t} F(t) = \frac{1}{\tau} \exp(-t/\tau). \tag{3}$$

Logarithmic Histograms

Histograms can also be constructed by choosing bins to have constant widths on the logarithmic time axis, as shown in Fig. 1 *C*. Such bins have constant relative width; for example, one bin in this figure ranges from 1.0 to 1.26 ms, while another bin ranges from 100 to 126 ms. We assume that the logarithmic x-axis arises from the transformation

$$x = \ln t. \tag{4}$$

Let the bin width on the x-axis have the (dimensionless) value δx, and let the lower limit of the leftmost bin be x_s. Then the ith bin will have the lower limit

$$x_i = x_s + i\delta x$$

which corresponds to the actual dwell time

$$t_i = t_s \exp(i\delta x),$$

where $t_s = \exp(x_s)$. The ith bin therefore corresponds to the range of time values

$$t_i \leq \mathbf{t} < t_i \exp(\delta x). \tag{5}$$

Blatz and Magleby (1986*a*) accumulated their data into such bins, however for displaying the data they corrected for the variable bin width by dividing each n_i by the width δt_i of each bin. By Eq. 1 this result is seen to be proportional to the pdf,

$$\frac{n_i}{\delta t_i} \simeq Nf(t_i + \delta t_i/2). \tag{6}$$

These values were plotted on log-log coordinates along with the theoretical pdf, which in Fig. 1 *B* is the sum of two exponentials.

The pdf for Logarithmic Histograms

Our approach is to display the logarithmic histograms directly, without the variable-binwidth correction of Eq. 6. Such a histogram is shown in Fig. 1 *C*, where the ordinate is simply the number of events in each bin. For comparison with theory, we compute the appropriate pdf for the logarithmic time axis by first transforming the probability distribution function and then differentiating it to obtain the new pdf. Starting with the exponential distribution function (Eq. 2) and transforming according to Eq. 4 we obtain the distribution $G(x)$,

$$G(x) = F[\exp(x)] = 1 - \exp[-\exp(x - x_0)], \tag{7}$$

where

$$x_0 = \ln(\tau),$$

the logarithm of the time constant.

The corresponding probability density function $g(x)$ is obtained by differentiating G with respect to x,

$$g(x) = \exp[x - x_0 - \exp(x - x_0)]. \tag{8}$$

If we define the "generic" pdf as

$$g_0(z) = \exp[z - \exp(z)]$$

then we can write $g(x)$ simply as

$$g(x) = g_0(x - x_0). \tag{9}$$

The function $g(x)$ has three properties that are useful for our purposes. First, from Eq. 9 it is clear that a change in the underlying time constant τ results only in a shift of the function along the x-axis, rather than a change of scale. Second, the maximum value of $g(x)$ occurs when $x = x_0$, i.e., at the logarithm of the time constant, where the value of g is e^{-1}. Third, this maximum value is independent of the time constant, unlike the pdf in the linear histogram (Eq. 3) where the maximum value varies as $1/\tau$.

For comparison of the histogram with a theoretical distribution, we find analogously to Eq. 1 that if the grand total number of events is N, the expectation for the number of events in the ith bin is, in the limit of small δx,

$$n_i \simeq N\delta x g(x_i + \mathrm{d}x/2). \tag{10}$$

If the distribution consists of a sum of m exponential components, the pdf takes the form

$$g(x) = \sum_{j=1}^{m} a_j g_0(x - s_j), \tag{11}$$

where s_j is the logarithm of the jth time constant, and a_j is the fraction of the total events represented by that component. The smooth curve in Fig. 1 *C* was computed as in Eq. 11 as the sum of two terms, and the resulting $g(x)$ was scaled according to Eq. 10 to allow direct comparison with the histogram values.

Square-Root Ordinate

For the evaluation of fits to experimental data it is useful to know the characteristics of the expected scatter of the experimental points. Let the number of entries $\mathbf{n}$ in a bin have the mean value n_0 and variance σ_n^2. Assuming that $\mathbf{n}$ follows Poisson statistics, the variance is equal to the mean,

$$\sigma_n^2 = n_0.$$

Thus when a histogram is plotted with a linear ordinate, the scatter is larger in the higher bins, as demonstrated by the upper panels in Fig. 1, *A* and *C* where the deviations between the theoretical and experimental bin heights are compared. On the other hand, plotting the histogram with a logarithmic ordinate, as in Fig. 1 *B*, results in the largest apparent scatter from the bins containing few entries. For Poisson-distributed bin heights the scatter takes on a constant size with the following transformation:

$$y = n^{1/2}, \tag{12}$$

where y is the plotted value, and n is the number of entries in a bin.

To demonstrate this property, consider an error bar corresponding to one standard deviation for a bin having expectation value n_0. The error bar would extend from n_0 to $n_0 + n_0^{1/2}$, which by the transformation of Eq. 12 is plotted as a bar of length

$$\begin{aligned}\delta y &= n_0^{1/2} - (n_0 + n_0^{1/2})^{1/2} \\ &= y_0[1 - (1 + 1/y_0)^{1/2}].\end{aligned}$$

Expanding the term in brackets as a Taylor series in y_0^{-1} and reaining the first-order term we obtain

$$\delta y \simeq y_0\left(\frac{1}{2y_0}\right) \simeq \frac{1}{2}. \tag{13}$$

This transformation therefore yields error bars that have a constant length, independent of n_0. This property is demonstrated in Fig. 1 *D*, where the upper panel shows the magnitude of the scatter along with the constant estimate for the standard deviation throughout the width of the histogram.

FITTING OF DISTRIBUTIONS

Maximum Likelihood Methods

The fitting of experimental sets of dwell-time measurements is typically done by maximizing the logarithm of the likelihood with respect to the set of fitting parameters, denoted here by Θ. The fit is based on assuming a particular form of the probability distribution of the t_j, usually a sum of exponential terms: in this case Θ represents the set of time constants and coefficients of the exponential components.

The likelihood is equal to the probability of obtaining a particular set of observed dwell times t_j, given the form of the distribution and the parameters, and is proportional to the product over the N observations

$$Lik = \prod_{j=1}^{N} f(t_j|\Theta),$$

where $f(t_j|\Theta)$ is the probability density function evaluated at t_j with the particular set of parameters Θ. Because the likelihood typically takes on very small values, numerical evaluation of its logarithm is preferable. In practice the log likelihood is also corrected for the absence of very short and very long intervals that are missed due to experimental limitations. With this correction the log likelihood is given, within a fixed constant, by (Colquhoun and Sigworth, 1983)

$$L(\Theta) = \Sigma \ln [f(t_j|\Theta)/p(t_{\min}, t_{\max}|\Theta)], \tag{14}$$

where the t_j are the N experimentally observed dwell times, and

$$p(t_{\min}, t_{\max}|\Theta) = \text{Prob}\,(t_{\min} \le t < t_{\max}|\Theta). \tag{15}$$

is the probability that dwell times fall within the range of experimentally measurable times characterized by $t_{\min}$ and $t_{\max}$, computed from the probability distribution with parameters Θ.

Binned Maximum Likelihood

The likelihood for binned data is the probability that a set of data results in a particular set of bin occupancies n_i. The log likelihood from binned data can be calculated as

$$L_b(\Theta) = \sum_{i=1}^{k} n_i \ln \left\{\frac{F(t_{i+1}|\Theta) - F(t_i|\Theta)}{p(t_s, t_k|\Theta)}\right\}, \tag{16}$$

where $F(t_i|\Theta)$ is the probability distribution evaluated at the lower bound t_i of the ith bin using the parameter values Θ, and $p(t_s, t_k)$ is, as before, the probability that the experimental dwell times fall within the range of the k bins in the histogram (Eq. 15),

$$p(t_s, t_k|\Theta) = F(t_s|\Theta) - F(t_k|\Theta)$$

Notice that for the binned data we use the probability distribution function $F(t)$ in the calculations, rather than the probability density (pdf) as in Eq. 14. We evaluate $F(t)$ at each bin edge and take the difference; this gives the probability that an event falls in the bin. Taking this difference is equivalent to integrating the pdf over the width of the bin.

Maximum likelihood estimation from binned data is equivalent to the unbinned estimation as in Eq. 15 in the limit of small bin width. From Eqs. 1, 14, and 16 it can be shown that:

$$L_b(\Theta) \simeq L(\Theta) \sum_{i=1}^{k} n_i \ln (\delta t_i), \tag{17}$$

where δt_i is the width of the ith bin; equality holds in the limit of small δt_i. Since in the fitting problem the n_i and δt_i are constants and only the parameters Θ are varied, the particular Θ that maximizes L will also maximize L_b.

For a sum of m exponential components the probability distribution function takes the form

$$F(t|\Theta) = 1 - \sum_{j=1}^{m} a_j \exp(-t/\tau_j), \tag{18}$$

where Θ consists of the entire set of the coefficients a_j and time constants τ_j. Each a_j represents the fraction of the total number of events contained in the jth component, and these coefficients sum to unity,

$$\sum_{j=1}^{m} a_j = 1$$

so that the set of parameters Θ has $2m$-1 independent elements. Maximum-likelihood fitting of the binned data then consists of finding the set of parameters Θ that maximizes $L_b(\Theta)$.

STATISTICAL ERRORS IN FITTING BINNED DATA

Sine and Steinbach (1986) and McManus et al. (1987) have considered two kinds of systematic error in estimating kinetic parameters that arise from discrete sampling and binning of data. First, there is an error in the estimates of brief exponential components when the event durations are measured as discrete multiples of a sampling interval. In our laboratory we use the 50%-threshold-crossing technique for estimating event durations, but we interpolate the experimental current trace data in the vicinity of threshold crossings (Colquhoun and Sigworth, 1983). The resulting dwell-time estimates are not quantized, so that this source of systematic error does not arise. (It should however be noted that there remains a more subtle problem of random errors in dwell-time estimates that arise from noise in the current trace. This sort of error was considered in Colquhoun and Sigworth, 1983, and is expected to be small.)

Second, McManus et al. (1987) have pointed out a "binning error" that occurs when bin heights are compared with theoretical probability density values. This systematic error can be understood from the approximations (Eqs. 1 and 10) that relate the bin heights to the pdf values at the bin centers: the approximations become poor when the bin width increases to become comparable to the time constants in the pdf. We have presented here a simple solution to this problem, namely to use the probability distribution function, rather than the probability density, in the maximum likelihood evaluation (Eq. 16).

Having dealt with these two sources of error, we wanted to see how wide the bins could be made without introducing other errors into the estimation of parameters by the binned maximum likelihood method. The process of collecting events into bins inevitably removes some information from the data. One therefore expects that at larger bin widths the parameters should show additional scatter that reflects the loss of information. To characterize these errors we used the maximum likelihood technique to estimate parameters from groups of 100 synthetic data sets. Each data set was created using the same values of time constants and numbers of events but were generated with different random numbers. From the 100 sets of estimated parameters so obtained, we computed the standard deviation and mean values for comparison with the starting parameters used in constructing the data sets. The process of maximum-likelihood estimation was repeated using densities of bins ranging from 2 to 64 bins per decade (corresponding to δx = 1.15 to 0.036). In some cases we also subjected the data sets to the direct log-likelihood evaluation (involving no binning; Eq. 14), to test the dependence of the errors on the binning procedure. In these simulations we used a variety of starting parameters and different numbers of events ranging from N = 1,024 to 25,600 in order to pose both well-conditioned and ill-conditioned fitting problems.

METHODS

Synthetic data in the form of exponentially distributed random numbers were obtained by taking the logarithm of the output of the FORTRAN-77 RND function on our PDP-11/73 computer (Digital Equipment Corp., Marlboro, MA). This RND function uses a 32-bit algorithm and has a period much longer than the size of our data sets. The resulting random numbers were scaled and pooled according to the time constants and amplitudes of the distribution to be simulated, and synthetic dwell times smaller than $t_{min} = 10^{-5}$ s were eliminated from the data set to simulate a detection limit. The events were collected into bins with widths given by Eq. (4) with $t_s = 10^{-5}$ s and $\delta x = 2.303/m$, where m is the number of bins per decade. The log likelihood was computed according to Eq. 16 for binned data, or according to Eq. 14 for the unbinned maximum-likelihood (ML) estimation. The computations used 32-bit floating-point arithmetic and the floating-point buffer operations of BASIC-23. A simplex search procedure (Caceci and Cacheris, 1984) was used to maximize the log likelihood; for a typical three-component fit (five parameters) the roughly 200 iterations required 30 min for the unbinned ML estimation from 2,048 data points, but only 2 min when binning was used (16 bins/decade).

In each group of 100 fitting operations the mean μ_i and standard deviation σ_i was computed for each of the fitted parameters. As an overall measure of the fitting errors, root-mean-square values of the normalized standard deviation $\sigma'$and bias μ' were computed from the n_p parameters as

$$\sigma' = \left[\frac{1}{n_p}\sum_{i=1}^{n_p}\left(\frac{\sigma_i}{\nu_i}\right)^2\right]^{1/2}$$

$$\mu' = \left[\frac{1}{n_p}\sum_{i=1}^{n_p}\left(\frac{\mu_i - \nu_i}{\nu_i}\right)^2\right]^{1/2},$$

where ν_i is the theoretical value of the ith parameter, i.e., the value that was used in generating the synthetic data.

RESULTS

Effect of Bin Density on the Precision of Fitting.

We performed binned and unbinned maximum-likelihood fitting on data sets from eight different distributions containing two or three exponential components. For each of these underlying distributions we used two different numbers of events N. The greatest sensitivity to the effects of binning appeared, as might be expected, in the "ill-conditioned" problems where N was relatively small, and where the time constants were closely spaced or the amplitudes of components were small. Three distributions

of this kind are illustrated in the upper panels of Fig. 2, and the dependence of the rms errors on bin width is shown in the lower panels.

The fitting problem illustrated in Fig. 2 *A* was the most difficult one we tried. The distribution had time constants of 0.02, 1, and 10 ms and amplitudes of 0.2, 0.1, and 0.7, respectively. This problem exemplifies a common situation in which a component of intermediate time constant is "buried" between larger components; here the 1-ms component represented only 10% of the events, and is hardly visible in a plot of the composite distribution (Fig. 2 *A*, *top panel*). This component was also very difficult to fit: in the 100 data sets of 2,560 events, even the best binned fitting operation (at 16 bins/decade) yielded estimates of this time constant with a scatter (SD) of ±0.58 ms, and the 100 amplitude estimates had the mean and SD of 0.12 ± 0.041. The normalized, overall errors in fitting this distribution at a bin density of 16/decade were $\sigma' = 0.31$ and $\mu' = 0.13$.

In this distribution, and in general, the quality of fitting was surprisingly insensitive to the density of bins used. The scatter σ' (plotted as squares with solid lines in the lower panel of Fig. 2 *A*) declined with increasing bin density up to 8–16 bins/decade, beyond which it remained essentially constant. The bias parameter μ' (*squares with dashed lines*) continued to decrease as the bin density increased to 64 bins/decade; however, since the bias values were usually small compared with σ', changes in these values reflect only small effects on the quality of fits. This is because the expected standard error ϵ' of the parameters in a single fit depends on the sum of the squares of σ' and μ',

$$\epsilon' = (\mu'^2 + \sigma'^2)^{1/2}.$$

When the number of events was increased 10-fold to N = 25,600, the precision of the fitted parameters improved by roughly a factor of 3. The same general trends were apparent in the dependence of σ' (*triangles with solid lines*) and μ' (*triangles with dashed lines*) in Fig. 2 *A*, except that the bias effects due to binning were more prominent in this case because the large number of events makes the statistical errors smaller.

Fig. 2 *B* shows the corresponding results for another three-component distribution that posed better-conditioned fitting problems. The components had time constants of 1, 3, and 10 ms and relative amplitudes 0.3, 0.4, and 0.3, respectively. Again, the quality of fitting was only weakly dependent on bin density with no significant increase in the precision of fitting occurring beyond 16 bins/decade.

Fig. 2 *C* shows the results for two fitting problems

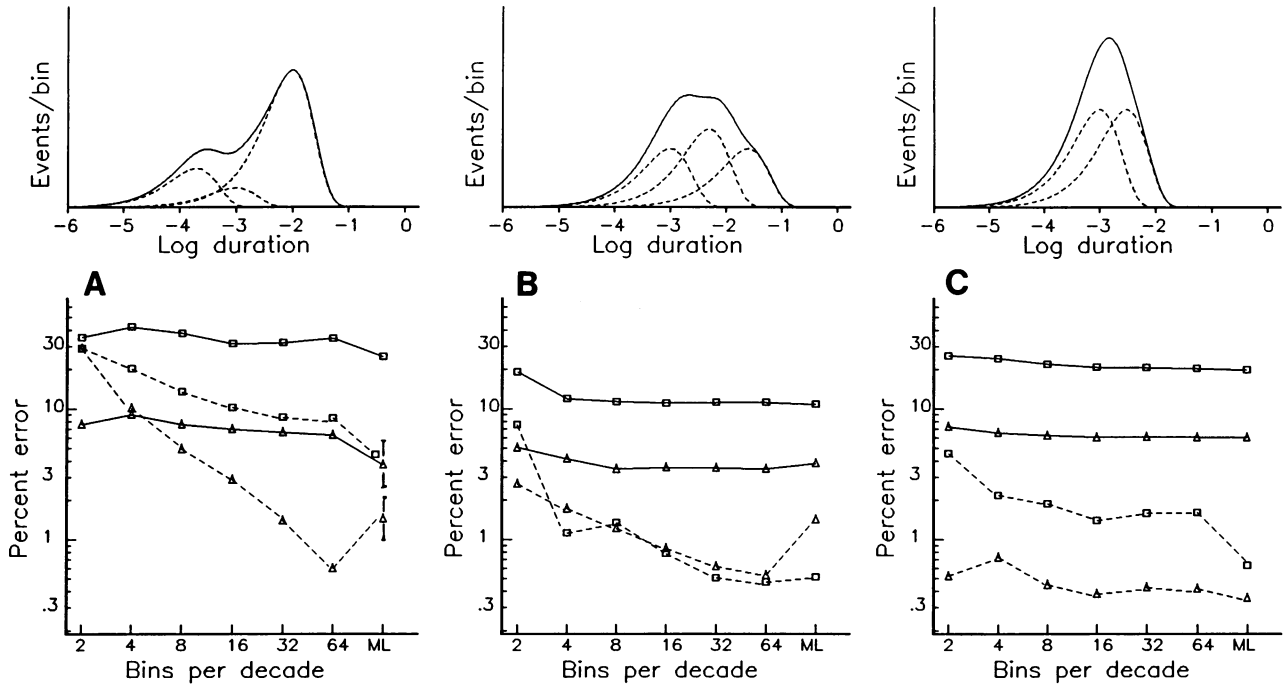

FIGURE 2 Dependence of fitting errors on the density of bins, as estimated from fitting groups of 100 synthetic data sets. The rms scatter σ' (*symbols with solid lines*) and bias μ' (*symbols with dashed lines*) are plotted as a function of bin density, given as bins per decade; ML indicates the results of unbinned maximum-likelihood estimation. The upper panels illustrate the distributions, plotted as in Fig. 1 *C* and Eq. 11. In *A*, the distribution consisted of three exponential components with time constants 0.02, 1.0, and 10 ms and amplitudes (i.e., fractions of total events) 0.2, 0.1, and 0.7, respectively. The squares represent parameters from fits to 2,560 data points, while the triangles were from fits to 25,600 data points. (Only 10, rather than 100, unbinned ML fits were performed for 25,600 points.) (*B*) Fits to a distribution with time constants of 1, 5, and 25 ms and amplitudes 0.3, 0.4, and 0.3. The squares are from 2,560 data points, the triangles from a total of 25,600 data points. (*C*) Fits to distributions with two components of equal amplitude. *Squares*, 1,024 points with time constants of 1 and 3 ms. *Triangles*, 1,024 points with time constants of 1 and 10 ms.

involving 1,024 events consisting of two exponential components. The squares represent errors in fitting a distribution having the two time constants separated by only a factor of 3 (shown in the top panel of Fig. 3 *C*); the triangles are from a distribution with time constants separated by a factor of 10. In each case there is remarkably little difference in the fitting errors between a bin density of 2/decade and the highest density used, 64/decade.

Comparison with Classical Maximum-Likelihood Fitting

The binned maximum-likelihood fitting, which required one to two orders of magnitude less computer time, nevertheless gave comparable results to the classical, unbinned maximum likelihood technique (indicated by ML in each part of Fig. 2). Asymptotically the binned and unbinned techniques are equivalent (Eq. 17) but they have different sensitivities to roundoff errors and therefore are expected to behave differently in practice. The largest difference between binned and unbinned fitting was seen in the runs of Fig. 2 *A*. The σ' and μ' values for the ML run with N = 25,600 are less precise because we performed only 10 of the 3-h fitting runs to compute them; however, both ML runs appeared to have slightly lower σ' values. In the other fitting problems tested, as in Fig. 2, *B* and *C*, essentially no difference was seen between unbinned fits and binned fits with densities of 16/decade or greater, and in some cases the ML fitting actually showed higher bias values, which is to be expected from the possible roundoff errors in accumulating the large sum (Eq. 14) that runs over the total number of events.

We conclude from these and other simulations that the binned fitting performs comparably to the unbinned maximum-likelihood estimation, and that relatively coarse binning can be used without introducing substantial errors. Little improvement in performance is seen from bin densities above 16/decade, and acceptable behavior is obtained at 8 bins/decade. Indeed, for two-component distributions as in Fig. 2 *C* the very coarse binning of 2/decade may be acceptable. We have standardized on a density of 10 bins/decade, which is the density shown in the logarithmic histograms of Figs. 1 and 3.

DISCUSSION

We have presented here a comparison of methods for displaying dwell-time histograms and have derived the form of the corresponding theoretical functions for the comparison of the histograms with exponential distributions. As the most useful representation of dwell-time data we suggest the display of histograms with a logarithmic time axis and a square-root vertical axis, as in Fig. 1 *D*. This display has a number of advantages over the traditional linear histogram display, including the properties that (*a*) exponential components appear as peaked func-

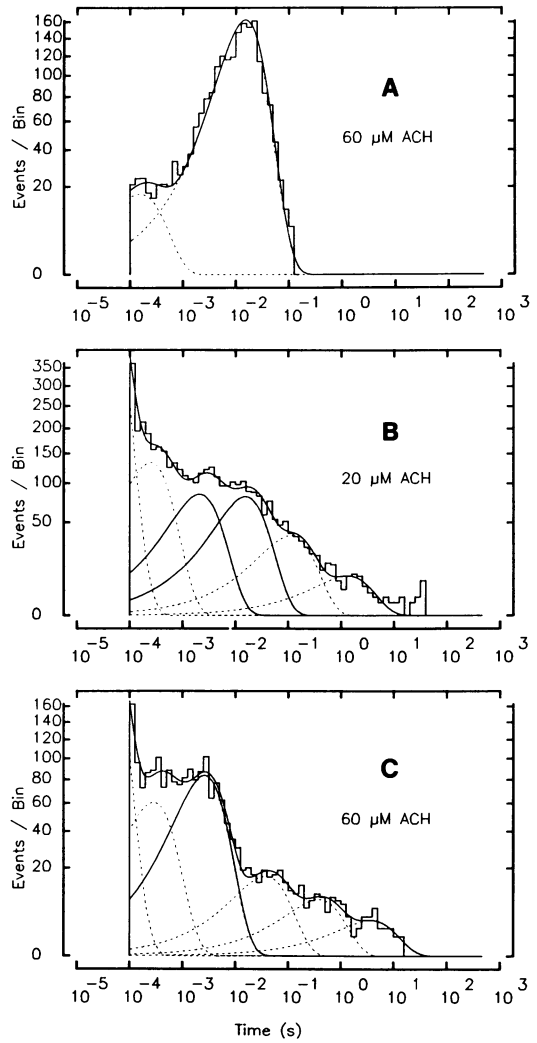

FIGURE 3 Histograms and fitted probability density functions from the data of Sine and Steinbach (1987). Recordings from cell-attached patches on BC3H-1 cells were made at 11°C and −70 mV patch membrane potential. (*A*) Open time distribution with 60 μm acetylcholine in the pipette, from 2,009 observed events. The fit predicts a total of 2,120 events, 9% of which are contained in a 160-μs component, and 91% in a component with a time constant of 15 ms. (*B*) Closed-time histogram at 20 μM ACh, from 4,065 observed events; same data as in Fig. 4 of Sine and Steinbach. Highlighted as solid curves, the equal sized components with time constants of 15.6 and 2.1 ms are associated with the effective channel opening rate and the agonist dissociation rate of the singly liganded receptor, respectively. The estimated time constants and fractions of events are: 1.32 s, 0.009; 113 ms, 0.036; 15.6 ms, 0.08; 2.1 ms, 0.08; 250 μs, 0.13; 33 μs, 0.66. (*C*) Closed-time histogram at 60 μM ACh, from the same recording as in *A*. The activation closures which were seen as two components at 20 μM ACh appear here as a single component (*solid curve*). The shift of the component is interpreted as resulting from an increase of the effective channel opening rate, in which the time constant decreases from 15.6 to 2.9 ms. The other component, associated with agonist dissociation, is predicted to take on a much smaller amplitude at 60 μM, and is apparently not visible here. The estimated number of events is 5,951; time constants and relative fractions of events are: 3.7 s, 0.007; 380 ms, 0.017; 38 ms, 0.033; 2.6 ms, 0.17; 290 μs, 0.12; 31 μs, 0.66. For a detailed description of the interpretation of the various components in the histograms, see Sine and Steinbach (1987).

tions in the display; (*b*) the position of the peak in each component corresponds directly to its time constant; (*c*) the height of each peak corresponds to the total number of events in that component; and (*d*) the expected statistical scatter in the data is of constant magnitude throughout this type of display.

We have also considered some issues in the fitting of distributions to logarithmically binned data. As Blatz and Magleby (1986*a*) and McManus et al. (1987) have pointed out, the binning of data can greatly accelerate the estimation of parameters using the maximum-likelihood method. McManus et al. (1987) found that bin densities as low as 25/decade are acceptable, but we conclude from simulations and from using an improved likelihood evaluation method that even lower bin densities (i.e., wider bins) can be used with little degradation in the quality of parameter estimation.

It should be noted that our concern here has been to optimally display and fit distributions of observed dwell times. We have not considered here the corrections necessary for interpreting these distributions and comparing them with theory in cases where a significant number of events are not resolved. Strategies for making such corrections have been discussed in the literature (Roux and Sauvé, 1985; Blatz and Magleby, 1986*a*).

Fig. 3 demonstrates the logarithmic display and the bin fitting techniques applied to dwell times recorded from acetylcholine receptor channels in BC3H-1 cells. The data are taken from the study of the agonist concentration dependence of closed and open durations described by Sine and Steinbach (1987). Simply plotting the dwell times on the logarithmic time scale reveals qualitative features of the distributions. The open time histogram (Fig. 3 *A*) consists of a major component with a peak near 15 ms plus a small component with a much briefer mean duration. The closed time distributions (parts *B* and *C* of the figure) span five decades of time. Raising the agonist concentration from 20 to 60 μM causes a general shift in the closed time distribution toward shorter durations. The logarithmic and square-root transformations combine to show the number of components required to fit each histogram. In both histograms a partially resolved shoulder is seen at short durations, and five more peaks are visible spaced about a decade apart. Thus the logarithmic abscissa and the square root ordinate make qualitative features of the data immediately apparent.

This kind of display also serves as a starting point for quantitative analysis of the dwell-time histograms. A reasonable description of the histogram can be obtained from a manual fit to the sum of exponentials. The resulting areas and time constants then become seed values for maximum likelihood fitting. Because the histogram entries are collected into only about 60 bins, the maximum likelihood estimation of parameters requires little computer time. Starting from a manual fit of the six components, the fits in Fig. 3, *B* and *C*, converged in <10 min using our BASIC-23 program. A further advantage of this display method is that the quality of the fit can be readily judged because the scatter is expected to have a constant amplitude across the histogram. For example, deletion of one of the six closed duration components would leave undefined a highly significant population of dwells.

We thank Dr. C. Methfessel for his FORTRAN translation of the simplex routine.

This work was supported by grant number NS-21501 from the National Institutes of Health.

Received for publication 27 March 1987 and in final form 12 July 1987.

REFERENCES

Austin, R. H., K. W. Beeson, L. Eisenstein, H. Frauenfelder, and I. C. Gunsalus. 1975. Dynamics of ligand binding to myoglobin. *Biochemistry.* 14:5355–5373.

Blatz, A. L., and K. L. Magleby. 1986*a*. Quantitative description of three modes of activity of fast chloride channels from rat skeletal muscle. *J. Physiol. (Lond.).* 378:141–174.

Blatz, A. L. and K. L. Magleby. 1986*b*. Correcting single channel data for missed events. *Biophys. J.* 49:967–980.

Caceci, M. S., and W. P. Cacheris. 1984. Fitting curves to data: the simplex algorithm is the answer. *Byte.* May 1984: 340–348.

Colquhoun, D., and A. G. Hawkes. 1983. The principles of the stochastic interpretation of ion-channel mechanisms. *In* Single Channel Recording. B. Sakmann and E. Neher, editors. Plenum Publishing Corp., New York. 135–175.

Colquhoun, D., and Sigworth. 1983. Fitting and statistical analysis of single-channel records. *In* Single Channel Recording. B. Sakmann and E. Neher, editors. Plenum Publishing Corp., New York. 191–264.

McManus, O. B., A. L. Blatz, and K. L. Magleby. 1988. Sampling, log, binning, fitting, and plotting durations of open and shut intervals from single channels. *Pfluegers Arch. Eur. J. Physiol.* In press.

Roux, B., and R. Sauvé. 1985. A general solution to the time interval omission problem applied to single channel analysis. *Biophys. J.* 48:149–158.

Sine, S. M., and J. H. Steinbach. 1986. Activation of acetylcholine receptors on clonal mammalian BC3H-1 cells by low concentrations of agonist. *J. Physiol. (Lond.).* 373:129–162.

Sine, S. M., and J. H. Steinbach. 1987. Activation of acetylcholine receptors on clonal mammalian BC3H-1 cells by high concentrations of agonist. *J. Physiol. (Lond).* 385:325–359.